Journal of Sound and Vibration 328 (2009) 382–395

Contents lists available at ScienceDirect

Journal of Sound and Vibration

journal homepage: www.elsevier.com/locate/jsvi

The applicability of the Moebius transformation to mechanical and acoustic impedance modifications

D.W. Herrin *, J. Liu, G. Sampath

Department of Mechanical Engineering, University of Kentucky, 521 CRMS Building, Lexington, KY 40506-0108, USA

ARTICLE INFO

Article history:
Received 23 February 2009
Received in revised form
7 August 2009
Accepted 10 August 2009
Handling Editor: C.L. Morfey
Available online 2 September 2009

ABSTRACT

The Moebius transformation maps straight lines or circles in one complex domain into straight lines or circles in another complex plane. This paper will demonstrate that the acoustic response will trace a circle in the complex plane for straight line or circular modifications to mechanical or acoustical impedance. This is due to the fact that the equations relating the acoustic response to the modification are in a form consistent with the Moebius transformation. This is demonstrated for series and parallel mechanical and acoustic impedances. The principles presented in this paper for the case of mechanical impedance are in essence equivalent to what has been termed the generalized Vincent circle by other authors. This paper shows that the principle is valid for multiple excitation problems while also showing the applicability of the principle to acoustic impedance. The key qualifications for applying the Moebius transformation to mechanical and acoustic impedances is that the problem should be linear, and the impedance modification should be in one coordinate direction and at one position. The principle is shown to be valuable for understanding the effect of acoustic impedance modifications in waveguides. The principle is illustrated for several examples including a point excited plate, a construction cab, and an acoustic waveguide.

1. Introduction

The acoustic response (sound pressure at the driver's ear or some other important location) can often be suppressed by changing the mechanical or acoustic impedance at positions of high energy transmission (e.g. mount locations) although successful impedance modifications can also be introduced at positions that are less intuitive. Changing the mechanical impedance is inclusive of the addition of springs, masses, and/or dashpots at a single position or between two positions. Similarly, acoustic impedance can be modified by the addition of absorbing material or perforated material, or by changing the length of side branches.

Certainly, there are design rules in place to guide the selection of these impedance modifications for many problems [1–2]. Additionally, numerical optimization has been successful. Nevertheless, it is believed that the principle described in this paper can add insight when making design changes. Certainly, the principle described aids in understanding the effect of changing either mechanical or acoustic impedance. Additionally, the method described provides a simple technique for determining which positions are best for adding impedance modifications.

* Corresponding author. Department of Mechanical Engineering, College of Engineering, 151 RGAN Building, Lexington, KY 40506-0503, USA.
E-mail address: dherrin@engr.uky.edu (D.W. Herrin).

0022-460X/$ - see front matter © 2009 Elsevier Ltd. All rights reserved.
doi:10.1016/j.jsv.2009.08.009

The Moebius transformation can be expressed as

$$Z = \frac{\alpha z + \beta}{\gamma z + \delta} \tag{1}$$

where α, β, γ, and δ are complex numbers. This maps a straight line or circular modification of z in the complex plane resulting in a straight line or circle of Z when traced in the complex plane [3].

This principle has in fact been applied to vibration suppression problems. It has been termed the Vincent circle [4–6] and has proven useful as guide for mass, stiffness and damping modifications. It is applicable to any linear structural system excited harmonically. Discovered by Vincent [4] of Westland Helicopters in 1972, it was apparently overlooked in the intervening years until a recent paper by Tehrani et al. [5]. Vincent had noted that introducing a stiffness modification and varying the stiffness from minus to plus infinity would result in a circle when the displacement response was plotted in the complex plane. Vincent limited his scope to structures excited at a single point with a one-dimensional spring added between two positions on a structure.

Tehrani et al. [5] made an important contribution by discovering that the principle could be generalized to a dynamic stiffness modification in one dimension thereby including mass and damping modifications. Actually, a dynamic stiffness can also be thought of as a mechanical impedance modification and will be considered such in this paper. They noted that the vibratory response at any point will trace a circle as the real or imaginary part of the dynamic stiffness is varied from minus to plus infinity. This amounts to a straight line modification of the dynamic stiffness in the complex plane.

Applying the principle, the entire response region can be described for a structural modification introduced between two points or between a single point and ground. To the authors' knowledge, the usage of Vincent's circle had previously been limited to vibration suppression problems [4–7], and has been proven valid for structural loads, dynamic stiffness modifications and vibratory responses. The work described here demonstrates that the principle can be generalized for both mechanical and acoustic impedance modifications and acoustic responses.

The development for mechanical impedance will be reviewed in light of the fact that it is unfamiliar to most in the NVH (noise, vibration, and harshness) community. This paper will then demonstrate how the Moebius transformation can be utilized for:

- Visualizing the change in acoustic response due to an impedance modification.
- Multiple excitation problems.
- One-dimensional structural and acoustic impedance modifications (in series or in parallel) at a single position.

2. Application to mechanical impedance

The development of the method below is similar to that shown by Done and Hughes [6]. Fig. 1 shows a schematic of a structure with a modification between points r and s. The structure is excited at a point p and the response will be computed at a point q. Done and Hughes supposed that point q was on the structure and the response was a structural vibration. However, the derivation in this paper will assume a structural force at point p and an acoustic response at a point q. Note that in the derivation shown below, there is nothing that precludes the excitation at point p as being structural. It is only essential that the structure be excited harmonically with F_P being the complex amplitude of the force. Note also that point p could be located in the acoustic domain and the excitation could be acoustical (i.e. a monopole).

Assume that the spring is replaced by two forces F_r and F_s. In that case, the vibrational responses at points r and s in the direction of the mechanical impedance, and the acoustic response at point q can be written in terms of the applied forces F_p, F_r, and F_s. Thus,

$$p_q = H_{qp}F_p + H_{qr}F_r + H_{qs}F_s \tag{2a}$$

$$v_r = H_{rp}F_p + H_{rr}F_r + H_{rs}F_s \tag{2b}$$

$$v_s = H_{sp}F_p + H_{sr}F_r + H_{ss}F_s \tag{2c}$$

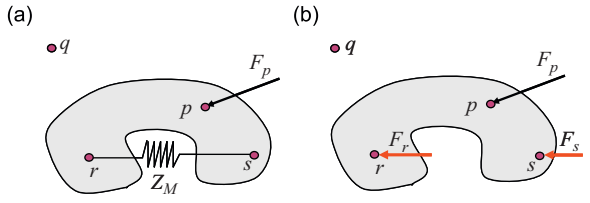

Fig. 1. (a) Schematic showing excited structure and location of modification. (b) Schematic showing the mechanical impedance replaced by forces.

where H_{ij} are the unmodified transfer functions (determined prior to any impedance modification) between the vibrational (velocity) or acoustic responses at point i and the forces or acoustical inputs at point j.

Note that the forces F_r and F_s can be expressed in terms of the mechanical impedance Z_M and the velocity responses v_r and v_s as

$$F_r = Z_M(v_s - v_r) = -F_s \tag{3}$$

and then substituted into Eq. (2). This results in a set of three simultaneous equations with three unknown responses x_r, x_s, and p_q. Solving for the modified transfer function (p_q/F_p), the following expression is obtained:

$$\frac{p_q}{F_p} = H_{qp} + \frac{Z_M(H_{sp} - H_{rp})(H_{qr} - H_{qs})}{1 + Z_M(H_{rr} + H_{ss} - H_{rs} - H_{sr})} \tag{4}$$

Tehrani et al. [5] observed that Eq. (4) is a particular case of the Moebius transformation.

Eq. (4) can be written in the form

$$a = b + \frac{Z_M c}{1 + Z_M d} \tag{5}$$

where a, b, c, and d are complex numbers defined as

$$a = \frac{p_q}{F_p} \tag{6a}$$

$$b = H_{qp} \tag{6b}$$

$$c = (H_{sp} - H_{rp})(H_{qr} - H_{qs}) \tag{6c}$$

$$d = (H_{rr} + H_{ss} - H_{rs} - H_{sr}) \tag{6d}$$

Tehrani et al. [5] further noted that the complex constants a, b, c, and d in Eq. (5) can be related to the complex constants α, β, γ, and δ in Eq. (1) via

$$\alpha = bd + c \tag{7a}$$

$$\beta = b \tag{7b}$$

$$\gamma = d \tag{7c}$$

$$\delta = 1 \tag{7d}$$

where the modified quantities a and Z_M (Eq. (5)) correspond to Z and z (Eq. (1)), respectively.

Done and Hughes showed that for a strictly real modification of Z_M, the radius ρ and center ξ of this circle can be expressed as

$$\rho = \left| \frac{c}{2\,\mathrm{Im}(d)} \right| \tag{8}$$

and

$$\xi = b - \frac{\mathrm{j}c\rho}{|c|} \tag{9}$$

respectively. Similarly, the radius ρ and center ξ of the circle can be expressed as

$$\rho = \left| \frac{c}{2\,\mathrm{Re}(d)} \right| \tag{10}$$

and

$$\xi = b + \frac{c\rho}{|c|} \tag{11}$$

for a strictly imaginary modification of Z_M.

Recall that mechanical impedance Z_M can be expressed as

$$Z_M = c_D + \mathrm{j}\left(-\frac{k}{\omega} + \omega m \right) \tag{12}$$

where k, m and c_D are stiffness, mass and damping, respectively. Thus, changing c_D or the quantity $-k/\omega+\omega m$ (i.e. the real or the imaginary part of Z_M) from minus to plus infinity will trace a circle in the complex plane. Note that this impedance modification is restricted to one direction. The minimum value of the complex modulus of a in Eq. (5) corresponds to the

minimum response for the modified system. Graphically, this is the point on the circle closest to the origin of the complex plane.

As an aside, it is notable that modifying the frequency in Eq. (12) results in a straight line modification of mechanical impedance in the complex plane. Eq. (12) is the system impedance for a single degree of freedom mass, spring, and damper combination. For viscous damping (proportional to velocity), it is well known that the mobility will trace a circle in the complex plane as frequency is varied for a single degree of freedom system [8]. Indeed, this is an example of a Moebius transformation. For hysteretic damping, it is the receptance which does so.

Likewise, plots of mobility for multiple degree of freedom systems will include sections of near-circular arcs in the vicinity of a natural frequency [8]. For a multi-degree of freedom system with viscous damping, a mobility transfer function (H_{pq}) can be written as

$$H_{pq} = \frac{A^r_{pq}}{c_r + \mathrm{j}\left(-\frac{k_r}{\omega} + \omega m_r\right)} + \sum_{\substack{s=1 \\ \neq r}}^{N} \frac{A^s_{pq}}{c_s + \mathrm{j}\left(-\frac{k_s}{\omega} + \omega m_s\right)} \tag{13}$$

where A^r_{pq} is the residue or modal constant linking coordinates p and q [8]; m_r, k_r, and c_r are the modal mass, stiffness, and damping, respectively, for mode r. For a narrow range of frequency in the vicinity of $\omega_r = \sqrt{k_r/m_r}$, the second term on the right hand side of Eq. (13) can be assumed to be independent of ω. In that case, Eq. (13) is analogous to the single degree of freedom case (Eq. (12)), and H_{pq} will trace an arc in the complex plane for a modification of ω. Ewins [8] terms this phenomenon the modal circle and this will be especially evident when the modal frequencies are well separated.

3. Series and parallel mechanical impedances

It is also interesting to consider the two separate cases where Z_M is replaced by two mechanical impedances Z_{M1} and Z_{M2} placed in series or in parallel. Utilizing the equivalence of Eqs. (1) and (5) shown earlier, Eq. (4) can be written in the form

$$\frac{p_q}{F_p} = \frac{\alpha_1 Z_M + \beta_1}{\gamma_1 Z_M + \delta_1} \tag{14}$$

where α_1, β_1, γ_1, and δ_1 are complex constants. Now, if Z_M in Eq. (14) is replaced by two mechanical impedances Z_{M1} and Z_{M2} placed in series so that

$$Z_M = \frac{Z_{M1} Z_{M2}}{Z_{M1} + Z_{M2}} \tag{15}$$

Eq. (13) can be written in the form

$$\frac{p_q}{F_p} = \frac{\alpha_2 Z_{M1} + \beta_2}{\gamma_2 Z_{M1} + \delta_2} \tag{16}$$

where

$$\alpha_2 = \alpha_1 Z_{M2} + \beta_1 \tag{17a}$$

$$\beta_2 = \beta_1 Z_{M2} \tag{17b}$$

$$\gamma_2 = \gamma_1 Z_{M2} + \delta_1 \tag{17c}$$

$$\delta_2 = \delta_1 Z_{M2} \tag{17d}$$

Note that Eq. (16) is in the form of the Moebius transformation shown in Eq. (1). Thus, the transfer function relating p_q to F_p will trace a circle in the complex plane for straight line modifications in the complex plane to either Z_{M1} or Z_{M2}.

A similar expression can be developed for the case of mechanical impedances in parallel. Replace Z_M by two mechanical impedances Z_{M1} and Z_{M2} in parallel so that

$$Z_M = Z_{M1} + Z_{M2} \tag{18}$$

Eq. (14) can be rewritten in the form of Eq. (16) where

$$\alpha_2 = \alpha_1 \tag{19a}$$

$$\beta_2 = \alpha_1 Z_{M2} + \beta_1 \tag{19b}$$

$$\gamma_2 = \gamma_1 \tag{19c}$$

$$\delta_2 = \gamma_1 Z_{M2} + \delta_1 \tag{19d}$$

Thus, modifying a particular mechanical impedance in a combination of series and parallel impedances will map the response or transfer function relating p_q to F_p to a circle in the complex plane.

4. Example—acoustic response due to an excited plate

The principle is illustrated via a plate with a single force excitation. Fig. 2 shows the geometry and the locations of the excitation, response and mechanical impedance. The thickness of the plate was 1.6 mm. Young's modulus, Poisson's ratio, and mass density were 200E9 N/m^2, 0.3, and 7850 kg/m^3, respectively. A spring-mass-damper modification was introduced at the point r. Numerical simulation was used to calculate the sound pressure (in air) at a point q due to a force applied at point p. A finite element model of the plate was created, and a forced response analysis was conducted to determine the vibration of the plate. Shell elements were used to simulate the plate. The plate was cantilevered on one side as shown in Fig. 2. The vibration response was subsequently used as the velocity boundary condition for a subsequent acoustic boundary element analysis. All simulations were performed at a frequency of 140 Hz.

The results are shown for two modifications in Fig. 3. Simulation results are indicated on the circle. The large circle is for a stiffness (k) and/or mass (m) modification with the damping (c_D) set to zero. This corresponds to varying the imaginary part of the mechanical impedance. Similarly, the smaller arc is for a damping modification (real mechanical impedance modification) with the stiffness and mass set to zero. Note that the circle and arc intersect at two points. One point occurs when all three constants (k, m, and c_D) are zero (i.e. the unmodified case). The other is when either k, m, or c_D is infinite. The smaller circle divides the larger circle into two separate arc lengths. The longer and shorter arc lengths correspond to stiffness and mass modifications, respectively, with the other set to zero. An optimum modification can be identified as that point where the response is a minimum (i.e. closest to the origin of the complex plane).

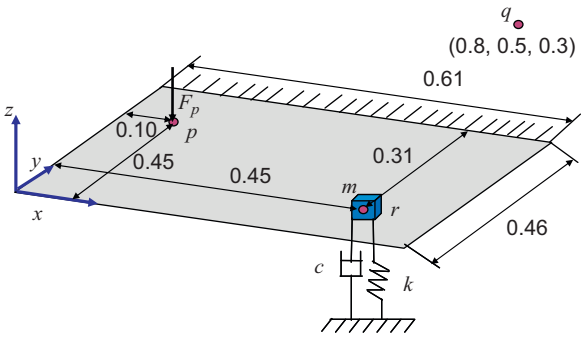

Fig. 2. Schematic showing cantilevered plate dimensions, location of the mechanical impedance, and point q for acoustic response. All dimensions and coordinates are in meters.

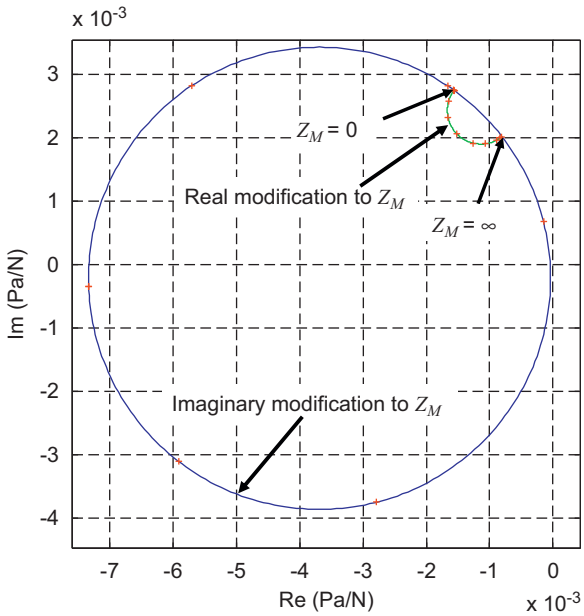

Fig. 3. Transfer function between pressure at point q and force at point p in the complex plane as a function of mechanical impedance. + indicates simulation results from finite and boundary element analyses.

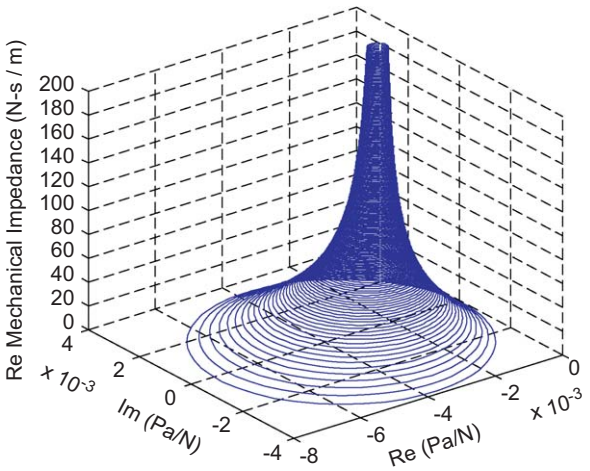

Fig. 4. Transfer function between pressure at point q and force at point p in the complex plane as a function of mechanical impedance. The real part of the mechanical impedance is varied along the vertical axis.

In Fig. 4, the damping is plotted on the vertical axis and a series of circles are traced in the different complex planes as the real part of the mechanical impedance (i.e. the damping) is increased. The circles have a smaller diameter for higher values of damping since damping tends to reduce the differences between resonances (i.e. occurring at a maximum distance from the origin of the complex plane) and anti-resonances (i.e. occurring at the minimum distance from the origin of the complex plane). As expected, the circles move towards the origin of the complex plane as the damping is increased.

5. Application to multiple excitations

The Moebius transformation can straightforwardly be extended to cases having multiple excitations in the following manner. Beginning with Eq. (4), the partial pressure response at point q due to a force or acoustic excitation at point n ($p_q^{(n)}$) can be written as

$$p_q^{(n)} = H_{qn}F_n + \frac{Z_M(H_{sn} - H_{rn})(H_{qr} - H_{qs})F_n}{1 + Z_M(H_{rr} + H_{ss} - H_{rs} - H_{sr})} \tag{20}$$

where F_n is a force at point n ($n = 1$–N). The complete pressure response p_q is the summation of the partial pressure responses and can be expressed as

$$p_q = \sum_{n=1}^{N} p_q^{(n)} = \sum_{n=1}^{N} \left(H_{qn}F_n + \frac{Z_M(H_{sn} - H_{rn})(H_{qr} - H_{qs})F_n}{1 + Z_M(H_{rr} + H_{ss} - H_{rs} - H_{sr})} \right) \tag{21}$$

Observe that Eq. (21) can be written in the form of Eq. (5) with

$$a = p_q \tag{22a}$$

$$b = \sum_{n=1}^{N} H_{qn}F_n \tag{22b}$$

$$c = \sum_{n=1}^{N} (H_{sn} - H_{rn})(H_{qr} - H_{qs})F_n \tag{22c}$$

$$d = (H_{rr} + H_{ss} - H_{rs} - H_{sr}). \tag{22d}$$

Eqs. (21) and (22) might not seem especially helpful at first glance due to the number of transfer functions which need to be evaluated to find b, c, and d if a large number of excitations are applied. However, the fact that Eq. (21) is of the form of Eq. (5) is potentially useful on its own. The complex constants b, c, and d can be solved for by making known modifications to the mechanical impedance (Z_M) to an analysis model or theoretically to an actual vibro-acoustic system. The constants b, c and d can be easily found by determining the responses for three known modifications to the mechanical impedance (Z_M).

Certainly, the aforementioned procedure could be applied experimentally. However, it is difficult to add a spring or mass to a real structure without also modifying the damping (i.e. the real part of the mechanical impedance). Furthermore, bolting a spring or mass to a plate adds rotational stiffness at the bolted location. Consequently, the authors' attempts to

prove this process experimentally have not been successful to this point. However, the approach could certainly be applied experimentally in principle, and Tehrani et al. [5] were successful in applying the principle to a beam.

6. Example—construction cab with multiple inputs

Finite and boundary element analyses of a construction cab were conducted, and the results were utilized to show how the Moebius transformation might be applied. Fig. 5 shows the finite element model of the construction cab as well as the approximate locations of the input forces at the four mounts and a mechanical impedance modification to the floor. The complex amplitudes for the four forces are indicated in Fig. 5 as well. The finite element model consisted 505 beam, 8852 shell, and 1778 solid elements. The finite element model for the cab was used to predict the structural vibration by a forced response analysis. Modal superposition was used for this analysis and 1 percent viscous damping was assumed for all modes.

The computed structural vibration was used for the velocity boundary condition for the subsequent boundary element analysis. The boundary element mesh consisting of 1640 elements for the construction cab is shown in Fig. 6. The absorption was applied (using a locally reacting model) to the indicated section of the construction cab. The impedance

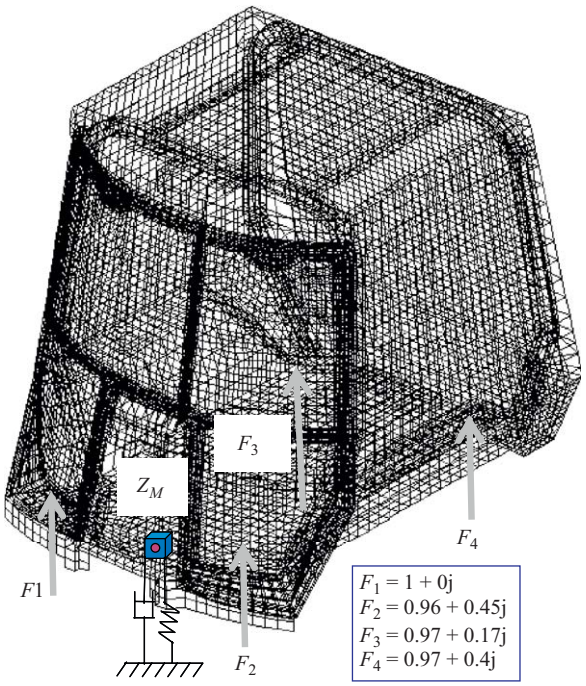

Fig. 5. Structural finite element model of construction cab.

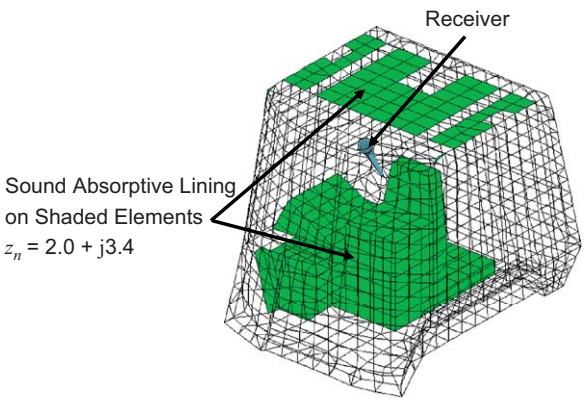

Fig. 6. Boundary element model of the construction cab showing location of absorption as shaded elements.

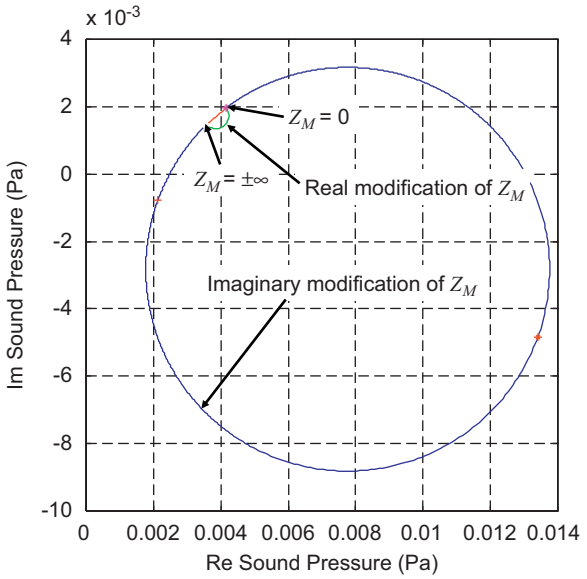

Fig. 7. Acoustic response plotted in complex plane at driver's ear location (140 Hz).

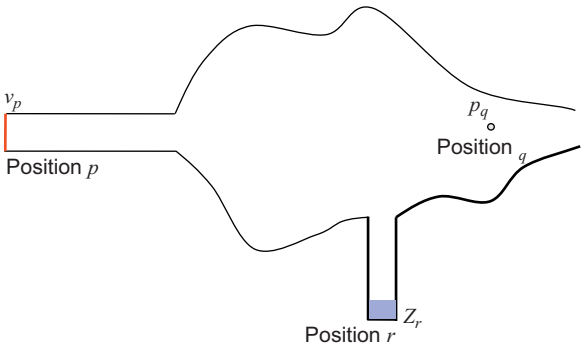

Fig. 8. Schematic to illustrate the application of the Moebius transformation to acoustic impedance.

corresponded to that of 1 in foam and the value for the local acoustic impedance at 140 Hz is shown in Fig. 6. The sound pressure response was computed at the location of the driver's ear.

Three finite and boundary element analyses were performed. The first was for the unmodified case and then two subsequent analysis cases were conducted where the imaginary part of the mechanical impedance was varied. The constants b, c, and d (Eq. (5)) were then determined using the results of these three simulations. The constants b, c, and d can be solved for since the three modifications (Z_M) and three corresponding responses p_q are known.

Computed circles in the complex plane for this example are shown in Fig. 7. The large circle is for an imaginary change to the mechanical impedance. This corresponds to a stiffness (k) and/or mass (m) modification with the damping (c_D) set to zero. The smaller arc is for a damping modification (real part of the mechanical impedance) with the stiffness and mass set to zero. The circles intersect at two points. One occurs when the mechanical impedance is zero (the unmodified case), and the other when either the real or imaginary part of the mechanical impedance is infinite. The longer arc length of the large circle corresponds to a mass modification with the stiffness and damping set to zero.

Several other simulations were conducted to demonstrate that the results lie on the circle and arc shown in Fig. 7 though these results are not indicated in the figure.

7. Application to acoustic impedance

The Moebius transformation may also be applied to acoustic impedance. This will be demonstrated using a development very similar to that shown earlier for mechanical impedance. Referring to Fig. 8, assume that a velocity source is applied (v_p) at position p and the response of interest is the pressure at point q (p_q). In this case, the modification is the

specific acoustic impedance at position r (Z_r). This analysis assumes plane wave behavior at the location of the specific acoustic impedance (position r) though not necessarily at points p or q.

The sound pressure at points q (p_q) and r (p_r) can be expressed as

$$p_q = H_{qp}v_p + H_{qr}v_r \tag{23a}$$

$$p_r = H_{rp}v_p + H_{rr}v_r \tag{23b}$$

where H_{ij} are the unmodified transfer functions between the sound pressure responses at point i and the particle velocities at point j. The particle velocity at position r (v_r) can be expressed in terms of the specific acoustic impedance as

$$v_r = \frac{1}{Z_r}p_r \tag{24}$$

When Eq. (24) is inserted into Eqs. (23a) and (b), one obtains

$$\frac{p_q}{v_p} = H_{qp} + \frac{\frac{1}{Z_r}H_{rp}H_{qr}}{1 - \frac{1}{Z_r}H_{rr}} \tag{25}$$

which has a form like Eq. (5) if Z_M is replaced by the reciprocal of Z_r. Similar to what was done for the mechanical impedance case, Eq. (25) can be re-expressed in a form similar to Eq. (1) as

$$\frac{p_q}{v_p} = \frac{\alpha\frac{1}{Z_r} + \beta}{\gamma\frac{1}{Z_r} + \delta} \tag{26}$$

If both the numerator and denominator on the right hand side of Eq. (26) are multiplied by Z_r, Eq. (26) will be in a form identical to Eq. (1). Thus, the response due to a straight line or circular modification to acoustic impedance likewise traces a circle in the complex plane.

Additionally, the Moebius transformation can be proven to be applicable to both series and parallel acoustic impedances using the identical analysis shown in Eqs. (14)–(19). In duct acoustics, series and parallel acoustic impedances are commonly denoted as transfer (used for modeling perforates) and branch (used for modeling side branches) impedances.

Fahy [9] noted that the specific acoustic impedances at positions (shown in Fig. 9) upstream (z_1) and downstream (z_2) could be related to one another via the expression

$$z_1 = \frac{z_2 + \mathrm{j}\tan(kL)}{\mathrm{j}\tan(kL)z_2 + 1} \tag{27}$$

where k is the acoustic wavenumber and L is the distance separating positions 1 and 2. Plane wave propagation of sound is assumed in the duct. Note that the expression is already in the form of the Moebius transformation (Eq. (1)) for both modifications of $\tan(kL)$ and z_2. Fahy previously demonstrated in Ref. [9] that z_1 traces a circle in the complex plane as $\tan(kL)$ varies from minus to plus infinity though not by utilizing the Moebius transformation. Similarly, it is apparent that if z_2 is modified along a straight line or circle, z_1 will similarly trace a circle in the complex plane according to the Moebius transformation.

Consider the case where the specific acoustic impedance z_0 is at the inlet or outlet to an acoustic duct system as shown in Fig. 10. Assuming that the duct system consists of a combination of series (indicated as z_{tr}), parallel (z_b), and termination or end (z_e) acoustic impedances, and straight ducts; z_0 will trace a circle in the complex plane due to any straight line or circular modification (in the complex plane) of any impedance in that system.

In the case of series impedance which is often referred to as transfer impedance, it is noteworthy that that Crocker and Sullivan [10] developed an empirical equation for impedance. The transfer impedance was expressed as

$$z_{tr} = \frac{6\times10^{-3} + \mathrm{j}k(t + 0.75d_h)}{\sigma} \tag{28}$$

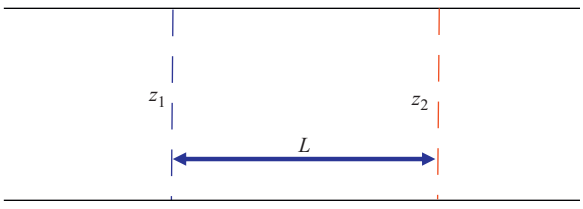

Fig. 9. Schematic showing impedance at two locations in a duct separated by length L.

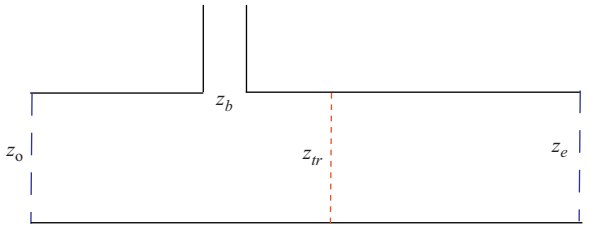

Fig. 10. Schematic showing a duct with a parallel (z_b) and series (z_{tr}) specific acoustic impedance.

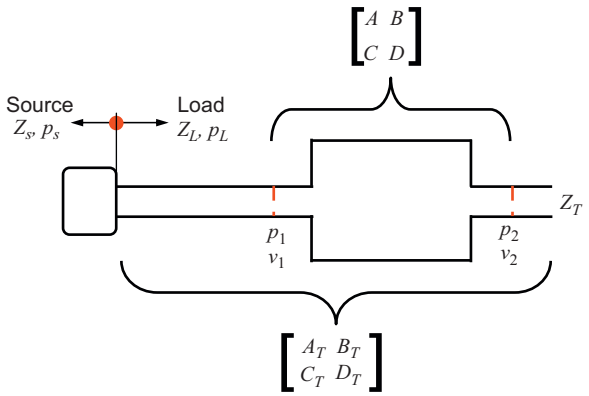

Fig. 11. Schematic illustrating the transfer matrix and source, load, and termination impedance.

where σ is the porosity, d_h is the hole diameter, and t is the thickness of the perforate. Rao and Munjal [11] developed a similar empirical equation which included the Mach number. Note that changing porosity (σ), hole diameter (d_h), or thickness (t) result in straight line changes to z_{tr} in the complex plane. In practice, these modifications will not extend from minus to plus infinity so only a portion of a circle will be traced. Maa [12] developed a similar transfer impedance expression for micro-perforates where both changing porosity and thickness though not hole diameter result in straight line changes in the complex plane.

An example of a parallel or branch impedance is a closed side branch (i.e. quarter wave tube). The specific acoustic impedance can be expressed as

$$z_b = -\mathrm{j}\rho c \cot(kL) \tag{29}$$

where L is the length of the closed side branch [12]. Note that varying the length will lead to a straight line modification of z_b. Similarly, the branch impedance of a Helmholtz resonator is

$$z_b = -\mathrm{j}\left(\rho\omega L' - \frac{1}{\omega}\frac{\rho c^2 S_B}{V}\right) \tag{30}$$

where L' is the equivalent length of the neck, V is the volume of the resonator and S_B is the area of the side branch [13]. Notice that modifying equivalent length, resonator volume, or side branch area produces a straight line change to the branch impedance.

8. Application to duct acoustics

Below, equations are developed for special applications to duct acoustics based on the transfer matrix methodology summarized by Munjal [13]. At lower frequencies, the duct cross-sectional dimensions are small compared to the acoustic wavelength. Accordingly, it can be assumed that plane waves propagate inside the duct system simplifying the analysis. In this case, a duct system can be described as an acoustic network using the well-known transfer matrix. The transfer matrix composed of four-pole parameters A, B, C, and D is defined according to the matrix equation

$$\begin{Bmatrix} p_1 \\ \rho_0 S_1 v_1 \end{Bmatrix} = \begin{bmatrix} A & B \\ C & D \end{bmatrix} \begin{Bmatrix} p_2 \\ \rho_0 S_2 v_2 \end{Bmatrix} \tag{31}$$

where p_1 and p_2 are sound pressures and v_1 and v_2 are particle velocities as defined in Fig. 11.

The four-pole parameters for certain components like rigid-walled straight pipes or ducts are well known [13]. However, numerical or experimental methods must be used to determine the four-pole parameters of more sophisticated

components like large expansion chambers and elbows in HVAC systems [14,15]. Fig. 11 shows a duct system including the source (Z_S) and termination impedance (Z_T). A_T, B_T, C_T, and D_T are the overall four-pole parameters including the effect of the inlet and outlet pipes.

The source pressure p_S can be related to load pressure p_L via

$$p_S = p_L\left(1+\frac{Z_S}{Z_L}\right) \tag{32}$$

where Z_S and Z_L are the source and load impedances, respectively. In turn, the load and termination impedances can be expressed as

$$Z_L = \frac{p_2}{\rho_2 S_2 v_2} \tag{33}$$

and

$$Z_T = \frac{p_1}{\rho_1 S_1 v_1} \tag{34}$$

By inserting Eqs. (32)–(34) into Eq. (31), the pressure at the termination (p_T which is identical to p_1) can be expressed as

$$p_T = \frac{p_S Z_T}{A_T Z_T + B_T + C_T Z_S Z_T + D_T Z_S} \tag{35}$$

where p_S is the source pressure. Note that Eq. (35) is already in the form of the Moebius transformation (Eq. (1)) for modifications to either source or termination impedance. If the modification is for source impedance, the complex constants identified in Eq. (1) can be expressed as

$$Z = \frac{p_T}{p_S} \tag{36a}$$

$$\alpha = 0 \tag{36b}$$

$$\beta = Z_T \tag{36c}$$

$$\gamma = C_T Z_T + D_T \tag{36d}$$

$$\delta = A_T Z_T + B_T. \tag{36e}$$

Similarly, if the termination impedance is modified, the complex constants can be expressed as

$$Z = \frac{p_T}{p_S} \tag{37a}$$

$$\alpha = 1 \tag{37b}$$

$$\beta = 0 \tag{37c}$$

$$\gamma = A_T + C_T Z_S \tag{37d}$$

$$\delta = B_T + D_T Z_S \tag{37e}$$

Furthermore, the Moebius transformation is also directly applicable to a series or branch impedance inserted into a duct system as shown in Fig. 12. In that case the pressure and particle velocity on the inlet side (indicated by the subscript 1) of

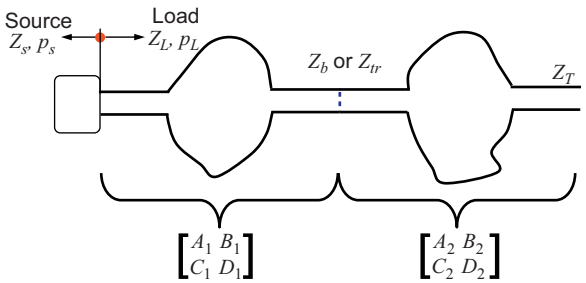

Fig. 12. Schematic showing a parallel (Z_b) or series acoustic impedance (Z_{tr}) inserted into a acoustic duct system.

the panel can be related to that at the outlet (indicated by the subscript 2) by

$$\begin{Bmatrix} p_1 \\ \rho_0 S_1 v_1 \end{Bmatrix} = \begin{bmatrix} 1 & Z_{tr} \\ 0 & 1 \end{bmatrix} \begin{Bmatrix} p_2 \\ \rho_0 S_2 v_2 \end{Bmatrix} \tag{38}$$

for a series impedance Z_{tr}, and by

$$\begin{Bmatrix} p_1 \\ \rho_0 S_1 v_1 \end{Bmatrix} = \begin{bmatrix} 1 & 0 \\ Z_b & 1 \end{bmatrix} \begin{Bmatrix} p_2 \\ \rho_0 S_2 v_2 \end{Bmatrix} \tag{39}$$

for a parallel impedance Z_b. The four pole parameters for the duct work to the left of the series or parallel impedance is given as A_1, B_1, C_1, and D_1 and to right of the impedance as A_2, B_2, C_2, and D_2. The overall four-pole parameters (A_T, B_T, C_T, and D_T) can be determined by multiplying the transfer matrices together. Then after inserting into Eq. (35), the transfer function relating p_T to p_S can be expressed in the form of the Moebius transformation (Eq. (1)) with

$$Z = \frac{p_T}{p_S} \tag{40a}$$

$$\alpha = 0 \tag{40b}$$

$$\beta = Z_T \tag{40c}$$

$$\gamma = A_1 C_2 Z_T + A_1 D_2 + C_1 C_2 Z_S Z_T + C_1 D_2 Z_S \tag{40d}$$

$$\delta = (A_1 A_2 + B_1 C_2) Z_T + (A_1 B_2 + B_1 D_2) + (C_1 A_2 + C_2 D_1) Z_S Z_T + (C_1 B_2 + D_1 D_2) Z_S \tag{40e}$$

for a series impedance. Similarly, the transfer function relating p_T to p_S for a parallel or branch impedance can be expressed in the form of Eq. (1) with

$$Z = \frac{p_T}{p_S} \tag{41a}$$

$$\alpha = Z_T \tag{41b}$$

$$\beta = 0 \tag{41c}$$

$$\gamma = (A_1 A_2 + B_1 C_2) Z_T + (A_1 B_2 + B_1 D_2) + (C_1 A_2 + C_2 D_1) Z_S Z_T + (C_1 B_2 + D_1 D_2) Z_S \tag{41d}$$

$$\delta = A_2 B_1 Z_T + B_1 B_2 + A_2 D_1 Z_S Z_T + B_2 D_1 Z_S. \tag{41e}$$

9. Example—acoustics of a duct system

The application of the Moebius transformation is demonstrated on the duct system shown in Fig. 13. Dimensions are shown in the figure. The duct system consists of source, termination, transfer, and branch impedances. The fluid was assumed to be air with a characteristic impedance of 415 Rayls. Plane wave behavior was assumed and all responses were computed making use of transfer matrix theory. All analyses were conducted at 1000 Hz.

The transfer function between p_t and p_s for a source impedance modification is shown in Fig. 14. The real part of the source impedance was modified from minus to plus infinity while the imaginary part was held constant ($-\rho c/\sqrt{2}$). Source impedance can be classified as a series impedance. Notice that transfer function between p_t and p_s traces a circle in the complex plane. Similar results were obtained for straight line modifications to termination impedance, and branch and series impedances.

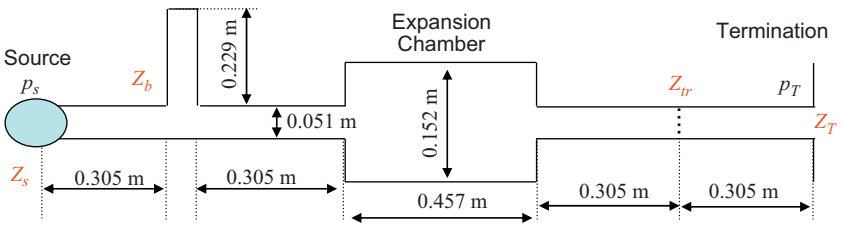

Fig. 13. Duct system including dimensions utilized for demonstration of Moebius transformation. Assume that all ducts are circular in cross-section.

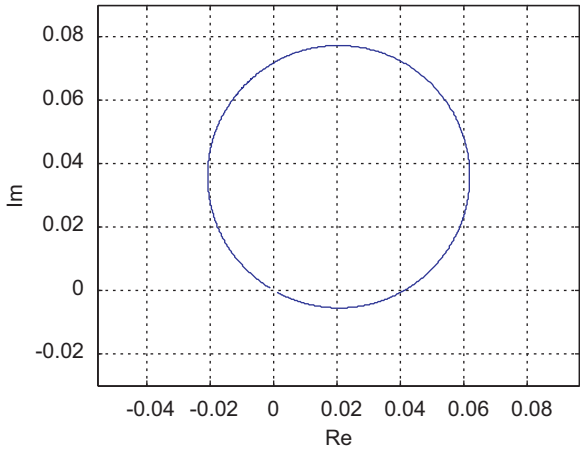

Fig. 14. Transfer function between p_t and p_s plotted in the complex plane for a real modification to source impedance (z_s) for the waveguide shown in Fig. 13.

10. Discussion

It has been demonstrated that the Moebius transformation—which maps straight lines and circles in one complex domain to circles in another complex domain—is a mathematical tool that can be employed to aid in determining and understanding the impact of mechanical and acoustic impedance modifications on a vibro-acoustic system. It was also demonstrated that the principle is suitable for multiple input problems.

Two vibro-acoustic examples were shown in the paper. The first demonstrated the validity of the principle for predicting the transfer function between sound pressure in the fluid and the force on a plate due to a mechanical impedance modification to the structure. The principle was also demonstrated for calculating the effect of a mechanical impedance change to the floor of a construction cab on the acoustic response at the driver's ear. It was shown that the principle was easily applied in numerical models. By finding the responses due to three separate modifications to the mechanical impedance, the entire response space for an impedance modification can be determined. It is believed that the principle could be exploited in numerical optimization problems.

Furthermore, the Moebius transformation is applicable to both series and parallel impedance modifications. This was shown to be especially enlightening for understanding the impact of impedance modifications to the response in waveguides. It was shown that the acoustic response will trace a circle in the complex plane due to straight line modifications to any impedance in a waveguide. It is believed that the method can be used to better understand the impact of modifying the impedances in ducts and provides a simple analysis tool for selected problems.

It should be noted that the application of the Moebius transformation is limited to single degree of freedom lumped element modifications. Certainly, this is a weakness to the approach. For example, a modification like changing the thickness of a panel could not be directly considered by means of the Vincent circle. In the case of duct acoustics, changing the length of an expansion chamber modifies impedance at two locations and the Moebius transformation is not directly applicable. However, Tehrani et al. [5] suggested that the Vincent circle still could be utilized in cases where there are multiple impedance modifications and researched visualizing Vincent circle results in such cases.

Similarly, the application of the Moebius transformation is limited to analysis at a single frequency. It is not advisable to use the approach if the structural or acoustic excitations are not tonal in nature since moving resonant frequencies will be of little benefit. That being the case, the methods are most applicable when anti-resonances can be assigned to important excitation frequencies. Fortunately, excitations are generally tonal for compressors, internal combustion engines, and many other sources of noise and vibration.

One drawback to the approach is that single degree of freedom lumped element modifications are difficult to implement in practice especially in the case of mechanical impedance. For example, the addition of a translational spring or damper generally also modifies the mechanical impedance in the other translational and rotational directions. Even if the impedance modification is precisely controlled, the local damping will likely be changed.

Nonetheless, the approach can be applied experimentally in principle. In fact, Tehrani et al. [5] successfully utilized the Vincent circle to minimize the structural vibration on a beam. Anti-resonances were identified using the Vincent circle and masses were added at selected locations. In practice, mechanical impedance is most easily controlled by changing the mass. If mass is welded to a structure, the change in damping (real part of the impedance) should be minimal compared to the change in mass (imaginary part of the impedance).

Though it may not be practicable to assign impedance precisely, knowing the optimal impedance has intrinsic value. For instance, by varying the impedance of a lumped element located on a panel, the impact of adding or subtracting mass, stiffness, or damping at a particular location can be assessed.

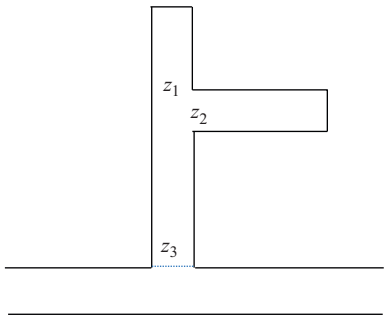

Fig. 15. Schematic showing side branch with parallel (z_1 and z_2) and series (z_3) impedances.

Acoustic impedance modifications in ducts are more easily controlled than mechanical impedances. As was previously noted, the method is amenable to any branch or series impedance modification. For the case of a side branch, the impedance can be most easily adjusted by adjusting the length (Eq. (29)). Likewise, the impedance of a Helmholtz resonator can be tuned by the equivalent length, resonator volume, and side branch area (Eq. (30)). Series impedances can be tuned in the case of perforates by their porosity, hole diameter and thickness as demonstrated in Eq. (28).

A potential application is shown in Fig. 15. In this case, a side branch extends from the main duct which includes a perforate and a connected side branch. Configurations similar to that shown in Fig. 15 are sometimes considered in industry due to space limitations or other design concerns. Notice that any of the impedances listed in the figure could be selected utilizing the Moebius transformation such that the acoustic response is optimized. After identifying the optimal impedance, impedance could be selected by selecting a suitable side branch length for z_1 or z_2. Similarly, the impedance of a series element like z_3 could be tuned by choosing appropriate perforate parameters.

Though this paper suggests several uses of the Moebius transformation for vibro-acoustics problems, it should be understood that the survey presented herein is by no means exhaustive. The authors suggest that this most useful mathematical principle could be applied in a number of other vibro-acoustic applications as well.

Acknowledgment

The authors are grateful for the support of the Vibro-Acoustics Consortium.

References

[1] ISO/TR 11688-2:1998, Acoustics—Recommended Practice for the Design of Low-Noise Machinery and Equipment—Part 2: Introduction to the Physics of Low-Noise Design, 1998.
[2] M. Bockhoff, Design of low noise machinery, in: M. Crocker (Ed.), *Handbook of Noise and Vibration Control*, Wiley, New Jersey, 2007, pp. 794–804 (Chapter 66).
[3] T. Needham, *Visual Complex Analysis*, Clarendon Press, Oxford, 1997.
[4] A.H. Vincent, A note on the properties of the variation of structural response with respect to a single structural parameter when plotted in the complex plane, Report GEN/DYN/RES/010R, Westland Helicoptors Ltd., September, 1973.
[5] M.G. Tehrani, W. Wang, C. Mares, J.E. Mottershead, The generalized Vincent circle in vibration suppression, *Journal of Sound and Vibration* 292 (3–5) (2006) 661–675.
[6] G.T.S. Done, A.D. Hughes, The response of a vibrating structure as a function of vibrating parameters, *Journal of Sound and Vibration* 38 (2) (1975) 255–266.
[7] C. Mares, J.E. Mottershead, Y.M. Ram, Numerical experiments with Vincent's circle, *Proceedings of the 22nd International Modal Analysis Conference*, Dearborn, MI, 2004.
[8] D.J. Ewins, *Modal Theory and Testing*, Research Studies Press, Letchworth, Hertfordshire, England, 1986.
[9] F. Fahy, *Sound in Waveguides, Foundations of Engineering Acoustics*, Academic Press, San Diego, 2001, pp. 181–235 (Chapter 8).
[10] J.W. Sullivan, M.J. Crocker, Analysis of concentric-tube resonators having unpartitioned cavities, *Journal of the Acoustical Society of America* 64 (1) (1978) 207–215.
[11] K.N. Rao, M.L. Munjal, Experimental evaluation of impedance of perforates with grazing flow, *Journal of Sound and Vibration* 108 (2) (1986) 283–295.
[12] D.-Y. Maa, Potential of microperforated panel absorber, *Journal of the Acoustical Society of America* 104 (5) (1998) 2861–2866.
[13] M.L. Munjal, *Acoustics of Ducts and Mufflers*, Wiley-Interscience, New York, 1987.
[14] D.W. Herrin, Z. Tao, E.L. Scalf, S.A. Allen, A.F. Seybert, Using numerical acoustics to predict the attenuation of HVAC plenums, *American Society of Heating, Refrigerating and Air-Conditioning Engineers Transactions* 113 (Part 1) (2007).
[15] D.W. Herrin, Z. Tao, A.E. Carter, J. Liu, A.F. Seybert, Using numerical methods to analyze multicomponent HVAC systems, *American Society of Heating, Refrigerating and Air-Conditioning Engineers Transactions* 113 (Part 1) (2007).